Automation in Construction 154 (2023) 104969

Contents lists available at ScienceDirect

Automation in Construction

journal homepage: www.elsevier.com/locate/autcon

Digital design and fabrication of clay formwork for concrete casting

Salma Mozaffari, Mackenzie Bruce, Gabrielle Clune, Ruxin Xie, Wesley McGee, Arash Adel *

University of Michigan, 2000 Bonisteel Blvd, Ann Arbor, MI 48109, USA

ARTICLE INFO

Keywords:
Clay extrusion
Formwork 3D printing
Additive manufacturing
Glass fiber reinforced concrete
Sustainability

ABSTRACT

This paper investigates the potential of clay extrusion as formwork for casting customized and building-scale fiber-reinforced concrete elements. Customizable shapes are produced using clay as cheap, sustainable, and easily demoldable formwork, extending its printable height limit. The coupled incremental clay 3D printing and concrete casting process allows the layered casts to start curing and reduces the hydrostatic pressure from concrete. The concluding case study, the Cocoon, demonstrates the method's capability to achieve building-scale height, integrate openings, and create complex surfaces. The introduced method seeks to challenge techniques and materials for 3D-printed formworks, demonstrating the ability to reduce the environmental impacts of concrete construction without compromising the complexity and time efficiency of bespoke elements.

1. Introduction

Addressing climate change requires significant innovations to reduce the carbon footprint of structures since the building industry contributes to more than one-third of global CO_2 emissions [1]. Concrete, by mass, is the most consumed material in the construction industry, and cement manufacturing, as the critical component of concrete, produces more than eight percent of the global human-made CO_2 emission [2]. Concrete requires support from formwork as it casts and transitions into solid, and formworks are significant contributors to the total cost of concrete construction, especially for non-standard elements [3–5]. Although the fabrication of bespoke and optimized concrete elements can avoid material waste, producing custom formworks with non-standard shapes is more wasteful and labor-intensive than traditional reusable formworks and, therefore, more costly [3,6,7].

Recent research in concrete and formwork fabrication through digital processes have incorporated technologies to reduce material waste and provide more freedom to produce non-standard building components [8–17]. This research investigates a manufacturing process for concrete structures coupling 3D printing of clay formwork with incremental concrete casting. The clay 3D printing for concrete casting is a novel technique providing recyclable and easily demoldable formwork and allowing the creation of building-scale bespoke concrete elements. The non-standard geometries created through this process (Fig. 1) are challenging, if not impossible, to fabricate using other advanced concrete casting technologies. Also, the demolding process (Fig. 2) for these complex geometries is effortless, and the material can be easily recycled and reused, strengthening its viability as a sustainable construction technique.

1.1. Background

Extensive research has been conducted on digital fabrication and additive manufacturing of concrete and clay. This section provides an overview of the most relevant research projects and summarizes the capabilities and drawbacks of each study.

Research on the digital fabrication of bespoke concrete elements can be divided into two categories of concrete casting; (1) using direct concrete 3D printing and (2) using a formwork or guide. 3D concrete printing (3DCP) can produce customized elements through the extrusion of concrete layers and was initially referred to as the *contour crafting* method [18]. The method has been investigated by several researchers and companies worldwide [6,19] and has successfully produced large-scale reinforced concrete structures [11,20,21], where unique aesthetics were explored through the articulation of surface and form. The method can integrate functional space for drainage, lighting channels, reinforcement, and alignment details. Although 3DCP is a nearly zero-waste method and efficient in time, problems have been reported regarding the layer adhesion between print layers [6,22], and increased drying shrinkage due to chemical admixtures and air exposure [23,24]. Also, it is more carbon- and energy-intensive due to the use of smaller aggregate size and higher binder content compared to traditional cast concrete [25,26].

The other category of digital concrete casting utilizes formwork or guides. Techniques for fabricating formwork include subtractive methods like Computer Numerically Controlled (CNC) milling and hotwire cutting [12,27], and additive formwork 3D printing methods

* Corresponding author.
E-mail address: aaadel@umich.edu (A. Adel).

https://doi.org/10.1016/j.autcon.2023.104969
Received 2 March 2023; Received in revised form 26 May 2023; Accepted 5 June 2023
Available online 19 June 2023

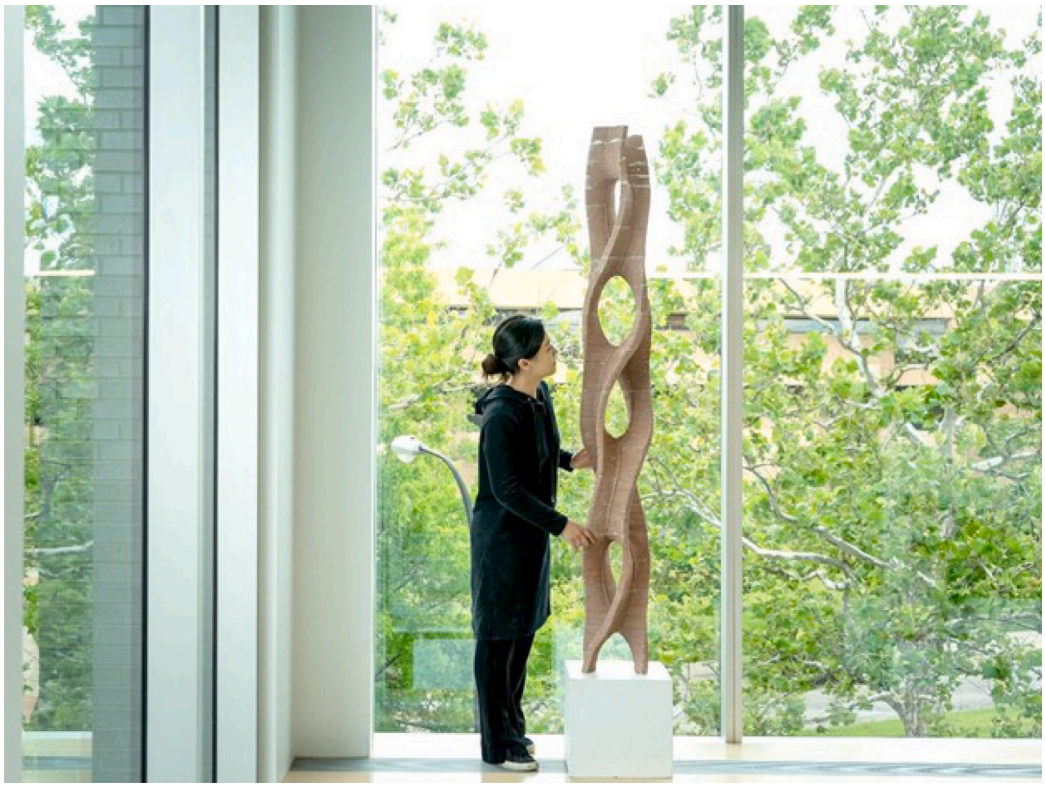

Fig. 1. Resultant concrete using 3D-printed clay formwork (the Cocoon).

Fig. 2. Final resultant cast after demolding (height = 1.3 m).

such as material extrusion, material jetting, and binder-jetting [28]. Examples of techniques using a guide include the *slipforming* technique of Smart Dynamic Casting (SDC) [9], spatial extrusion or reinforcing net in the Mesh Mould [8,29], and BranchMatrix [15] technologies. Of these techniques, the most relevant to this research is the formwork 3D printing using material extrusion, which will be reviewed along with other well-known techniques such as CNC milling and hotwire cutting, SDC, and Mesh Mould.

CNC milling and hotwire cutting of polystyrene foams is a commercially known subtractive method that starts with a block and cuts away portions to create custom forms [12,27,30]. As a result, it is materially wasteful. It cannot also integrate interior functionalities as opposed to 3DCP. Also, polystyrene has a complex recycling process [31]. The SDC technique [9,32] is a digitally controlled *slipforming* process that uses a set-on-demand concrete that enters a moving mold as a fluid and exits as a solid. However, due to the dynamic formwork, the method is limited in the range of shapes and cannot integrate openings. The Mesh Mould technique first utilized spatially extruded latticed polymer structures as reinforcement and a stay-in-place guide for concrete casting [8]. The polymer lattice structure was later replaced with robotically welded 3D steel mesh [29]. Although it does not incorporate voids and interior functionalities, the method has been promising in creating doubly-curved structural wall elements and offers more geometrical freedom than SDC. Nonetheless, the concrete surface requires manual finishing due to the absence of exterior formwork.

Formwork 3D printing through material extrusion commonly uses concrete and polymer. The 3D-printed concrete formwork usually acts as a *lost formwork* and does not have a load-bearing function [14,17,21]. The concrete is cast to the formwork after the outer shell hardens and gains strength. Although the method produces minimal waste, is time-efficient, accommodates reinforcement [20,21], and enables achieving significant heights using a fast-setting concrete [21], it could still carry the drawbacks of direct 3DCP, such as high drying shrinkage due to increased air exposure and high carbon emission if the aggregates are not selected carefully.

3D-printed polymer formwork using Fused Decomposition Modeling (FDM) was first proposed as an additive formwork method [33]. The method was further developed in other projects to produce geometrical freedom for concrete elements and to provide support lattice structures for the formwork [16,34–36]. The Eggshell project integrated conventional reinforcement into the method and used a fast-hardening set-on-demand concrete from the SDC project to reduce the lateral pressure on the formwork [5,13,37]. Although the formwork is reported to be recyclable and creates minimal waste, its removal requires a heat gun and could still include concrete particles after removal, making recycling difficult [5,38]. Also, Polylactic Acid (PLA) or other biodegradable plastics commonly used as filaments in FDM might not be fully recyclable as they could lose their mechanical properties after a few cycles [39].

The clay extrusion technique was first developed for contour crafting of ceramics [40]. Clay gains its plasticity when wet and becomes hard, brittle, and easily-washable when dry. The plasticity of clay allows it to be extruded for 3D printing in a continuous bead, similar to the traditional process of clay coil pots [41]. Therefore, when used as formwork, it is easily removable and washable. However, because of the clay's low resistance to hydrostatic pressure, casting concrete into clay formworks has demonstrated challenges. Wang et al. [42,43] have studied the clay's dryness level and deformation after concrete casting. Their process used a single concrete cast into dried and stacked clay sections. It was reported that bone-dry clay absorbs water from concrete, modifies its characteristics, and after a certain print height, the clay print structurally fails. The print length was also restricted and created a discontinuous process due to the loaded clay tube size used for extrusion.

This paper provides a more comprehensive scope and detailed explanation of the study previously summarized in Bruce et al. [44] by the authors. Our study shows a considerable improvement to the previous research on clay formworks [42,43] by using an incremental printing and concrete casting technique, allowing the cooperation of concrete and clay and providing scalability and customization opportunities.

1.2. Summary and problem statement

The previous section summarized relevant digital processes for manufacturing concrete elements and discussed their drawbacks. 3D printing through extrusion provides considerable geometrical freedom to create bespoke designs and enables the integration of openings for material saving and internal functional features, such as reinforcement and lighting. Therefore, they provide fewer limitations in the range of shapes compared to SDC and Mesh Mold technologies. Like 3D printing technologies, CNC milling and hotwire cutting can produce customized forms; however, they are very wasteful, have a complex recycling process, and typically cannot integrate interior functionalities.

A relevant drawback of concrete extrusion is that it has greater air exposure, which could cause excessive drying shrinkage and durability issues. Also, the aggregate size in the mixture is limited by the nozzle size, resulting in higher carbon emissions from using finer aggregates. Potential methods to compensate for higher carbon emissions include using recycled aggregates [45] and minimizing material usage [46]. Polymer printing uses biodegradable plastic, which can have a restricted life cycle and is not fully recyclable. Clay formwork has advantages over polymer as it is self-demolding when drying out. Other benefits of clay over concrete and polymer are lower costs and a smaller carbon footprint. Furthermore, clay's larger bead size is comparable to concrete 3D printing processes, allowing faster printing speeds as clay does not have to cure while printing.

Earlier studies on clay formworks observed extreme deformations during concrete casting and failed to achieve large scales or integrate openings and create branching structures. Therefore, combining the clay 3D printing process with concrete casting requires further investigations to achieve larger overhang geometries and provide more geometrical freedom. The study would be beneficial for utilizing a sustainable material as a customizable formwork producing creative architectural components, optimized forms, and structural elements by integrating functionalities such as reinforcing bars.

1.3. Objectives and contributions

This study explores the hypothesized advantages of using clay as formwork to investigate: (1) strategies to empirically control the hydrostatic pressure of concrete to achieve larger overhangs and building-scale prototypes, (2) its demolding and recycling potential, and (3) the accommodation of non-standard geometries, branching structures, and void integration that imposes irregular hydrostatic pressure.

The study contributes to the rapidly growing research on digital and sustainable manufacturing techniques for producing bespoke structural concrete elements. The state-of-art research on the digital fabrication of concrete has been moving towards the real-world construction industry [14,47,48]. However, several aspects, such as incorporating sustainability concerns, integrating into design guidelines, and achieving efficient production, have the potential for continuous research and further investigations. This research provides an improved understanding of clay performance as a sustainable material for formwork 3D printing coupled with concrete casting to create building-scale elements.

2. Materials and methods

The novel fabrication process introduces incremental clay printing and concrete casting allowing the formwork to reach higher scales than previously achievable (Fig. 3). To avoid wet clay deformation due to concrete's hydrostatic pressure and provide more stability for the formwork, the continuous casting process uses accelerators to reduce the curing time for concrete. To deliver scalability, concrete and clay work together and support each other. The fabrication method allows intricate details, undercuts, and openings, creating a wider range of geometries that are not easily achievable through 3DCP. Inspired by the advanced incremental concrete casting introduced through SDC [32], the devised method generates high-resolution material articulation similar to the 3D-printed concrete.

This section discusses the material formulation for the fast-hardening concrete and various clay types, the tooling and fabrication setup, as well as the experimental studies. The investigations rely on physical prototyping to tune the material composition and refine the fabrication process.

2.1. Materials

We explored various clay types, investigated a glass fiber concrete mixture with adjusted water quantity, and added an accelerator to introduce a robust process for deformation control and incremental clay 3D printing and concrete casting.

2.1.1. Clay

In the preliminary study, we investigated three clay types with high plasticity for deformation comparison. We hypothesized that the strength of highly plastic clay would limit its deformation due to hydrostatic pressure. The three clay types [49] with varying material compositions are: (1) The *RO-95 Cone 6 Porcelain* is a domestic kaolin-based, that does not contain Grolleg and has sodium flux, silica, and ball clay. (2) The *RO-01 You Betacha Mix* is a white porcelaneous clay including no sand and a three percent fine mullite grog. (3) The *RO-82M Terracotta* has most of the body content in redart as the iron-bearing clay, ball clay for plasticity, and mullite grog for smoother body and stability. All the clay types used in this study are purchased in a moist and printable condition, and according to the Atterberg limits [50], in a semi-solid/plastic range. More precise characterization

Fig. 3. Co-working environment between humans and robots, combining robotic clay printing and manual concrete casting processes.

of the clay water content, plasticity, density, and rheological properties is subject to further investigation.

2.1.2. Concrete mixture

The base concrete formula (courtesy of Prof. Tsz Yan Ng of Taubman College) consists of cement, ground silica, silica fume, water, polymer, superplasticizer, fine sand, and glass fibers creating a Glass Fiber Reinforced Concrete (GFRC). The base mixture is tested with adjusted water and varying accelerator (calcium aluminate cement) percentages to accommodate tube changing, printing time, and casting intervals. Similar to the recipe used in the Eggshell technique [13], the concrete mix used here is self-compacting, capable of flowing inside the formwork without segregation, did not usually show high porosity, and did not require vibration. A stand mixer is used to mix the formula in small batches, and two minutes before casting, the accelerator is added to the GFRC. The use of fibers could improve the load-bearing capacity of the mix [13]; however, the fibers alone do not guarantee sufficient strength or ductility [5]. They must be combined with other reinforcement strategies in future research to produce structurally functional elements.

2.2. Fabrication

2.2.1. Fabrication setup

Our fabrication setup (Fig. 4) comprises a 6-axis industrial robotic arm mounted on a linear track with a clay extrusion end effector. This section provides a detailed description of the setup.

Clay extrusion processes for additive manufacturing typically fall into three categories: piston extruders, progressive cavity pumps, and screw extruders [51,52]. Of these, the first two are considered positive displacement and therefore have a linearly proportional relationship between the piston's or rotor's input velocity and output flow. Progressive cavity pumps are limited in the maximum viscosity of the pumped material, with most manufacturers indicating a limit of less than 1,000,000cps [53]. To maximize the print buildability in this research, we used semi-solid clay. Piston extruders can effectively extrude semi-solid materials, given enough force, and the extrusion rate will be directly proportional to the velocity of the piston.

Piston extruders can be pneumatic, hydraulic, or screw-driven [52]. From a machine design standpoint, pneumatic and hydraulic pistons provide high forces, but they require relatively expensive linear encoders and servo-proportional valves to provide highly dynamic motion control. Electromechanically driven pistons utilize high precision, low friction ball or roller screws actuated by rotary servos. There are multiple factors to consider in the selection of either system. In this research, the piston is driven by a 16 mm ball screw driven by a rotary servo equipped with a low-backlash planetary gear unit (Fig. 5).

The design and sizing of a piston extrusion system involve balancing several factors. The piston diameter affects the overall force required, and the total mass of the end-effector is related to the robot payload, as well as the total volume of clay that can be loaded and the resulting length of a print. In this study, we used a robot system with a 120 kg payload, although we kept the end effector mass lower to allow easy lifting by two researchers. The overall length of the piston also influences the location of the end effector center of mass and the tool center point (TCP). The robot manufacturer provides guidelines on the limits to these values. The clay is loaded into a 75 mm diameter, 600 mm long tube in this research. A typical layer cross-section of 6 mm wall thickness by 2 mm height corresponds to approximately 220 m of extrusion length. This imposes a key constraint in the fabrication process development as the print needs to stop for a tube change when the extruder runs out of clay. Therefore, mixing and clay filling stations are adjacent to the print workcell to allow continuous filling and mixing. The printing, mixing, and clay-filling orchestration creates an incremental process that integrates the discussed constraints of the fabrication setup.

2.2.2. Digital design-to-fabrication workflow

We employed a custom computational design tool, Super Matter Tool (SMT) [54], which allows offline programming and simulation of the robotic deposition process. The tool is programmed in C# [55] and integrated as a plugin into the Computer-Aided Design (CAD) software, Rhinoceros 3D [56]. This integration enables a seamless connection between the digital design and robotic simulation.

This tool contains an integrated slicing algorithm with support for planar and nonplanar layers, as well as the encoding of variable extrusion and robot feed rates into the individual toolpaths. In this research, we used planar layers for extrusion. The tool accepts both mesh and boundary representations as geometric inputs. According to the step height for each layer specified by the user, planar intersections

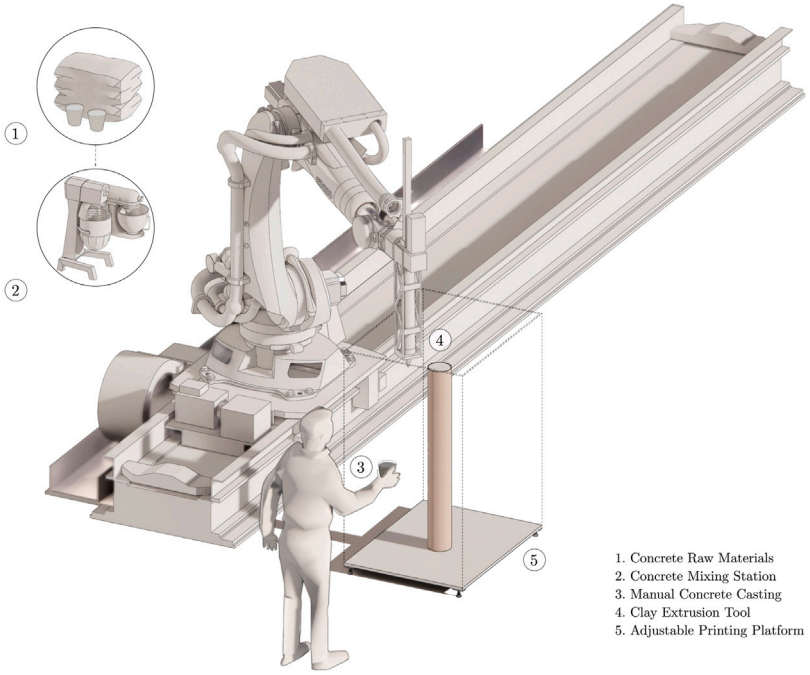

Fig. 4. Fabrication setup utilizing a 6-axis robotic arm with clay extruding end effector.

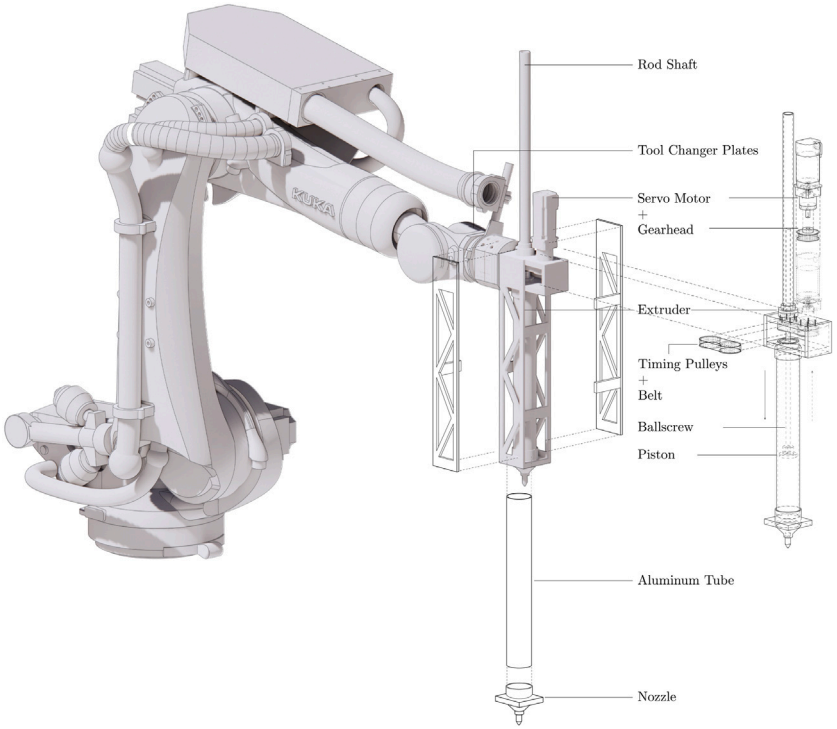

Fig. 5. Extrusion tool composition.

generate an array of contour curves, typically either Non-Uniform Rational Basis Spline (NURBS) or polyline. In the next step, each curve is subdivided into line segments according to the user-selected chord tolerance, defined as the maximum deviation of the new line segments from the original curve. These subdivisions are traversed to create an array of path waypoints, which store the information needed to generate machine instructions at a later step. This includes information such as the cartesian location of the waypoint, the parameter and segment information relative to the original curve, information about the extrusion rate and velocity of the end effector, as well as the TCP's orientation vector. In this research, the TCP is oriented vertically for the entire path. A user-selected subsequent step either connects the layers using short ramps (designated as *Planar* mode) or creates a continuous interpolated curve on the input geometry (designated as *Spiral* mode) to generate a continuous path. In the final step, the tool simulates the machine's kinematic motion and the approximate shape of the extruded part at every step. Additional machine-related settings like feed rate can be set, and based on the simulation results, specific kinematic

Fig. 6. From left to right: clay formwork, self-demolding dried clay, and resultant cast.

Fig. 7. From left to right: printing clay, demolded formwork, ground and separated formwork, and recycled printing clay.

parameters like end effector orientation can be modified or limited if necessary. This information is then automatically post-processed into Kuka Robot Language (KRL) [57] to generate machine instructions.

2.2.3. Control method

Extrusion-based additive manufacturing processes require a material deposition system whose extrusion rate can be precisely synchronized with the motion of the end effector (in the case of moving tool kinematics) or part (in the case of moving platform kinematics). Motion control platforms, such as six-axis industrial robotic arms and CNC machines, experience acceleration and deceleration phases as they follow their planned trajectory. This requires the extrusion system to precisely track the actual velocity of the end effector's TCP. Synchronization between the end-effector and the robot motion occurs through a software-based Programmable Logic Controller (PLC) motion controller. KRL supports up to 6 external axes, which can be virtual, allowing the robot controller to handle the synchronization of the robot and external axes, and passed via a real-time EtherCAT [58] interface to the external system, which handles the positioning of the end-effector axis. This approach enables low latency (<20 ms) control of external axes. Latency results in a *phase lag* between the robot's and the extruder's motion, resulting in under- and over-extrusion near corners and other areas of the path with variations in velocity, with the effect becoming more pronounced at higher end effector velocities. For example, with an end effector travel speed of 100 mm/s, a 20 ms time lag results in a spatial displacement of 2 mm, which is a reasonable tolerance at this scale.

2.2.4. Demolding and recycling

Incremental clay printing and concrete casting result in a curing concrete structure encased in clay. As the clay dries over 24–72 h, it shrinks and cracks, initiating self-demolding. Once the clay is dry, the formwork can be brushed away easily, requiring only a single laborer with no additional tools to complete the process (Figs. 2 and 6). This novel technique leverages the inherent material qualities of the clay. The clay can then be recycled through rehydration and filtered to be used again, harnessing the material properties as a nearly zero-waste option for concrete formwork (Fig. 7). Further testing is required to assess the material's potential and limitations for continuous recycling.

2.3. Experiments

The experiments were conducted in two phases of preliminary and deformation control, building up to a case study presented in Section 3.2 that applies the process to a large-scale and bespoke architectural element to test the developed method.

2.3.1. Preliminary studies

The first step of the initial experimentation compared the deformations of the printed clay cylinders with varying bead heights after concrete casting. The cylinders had 100 mm diameter, 250 mm height, and bead heights of 1 mm, 2 mm, and 3 mm (Fig. 8) with a wall thickness of 6 mm. We observed that the cast with 1 mm bead height results in the slightest deformation and least porosity (the trapped air is mostly on the external surface). Our test confirmed the results of past research [42], where the bead heights were tested and compared for deformation. We, therefore, used a 1 mm bead height for the rest of the experiments.

The second step compared the deformations of the three clay types discussed in Section 2.1.1, and the resulting concrete surface finish. Although terracotta clay has lower plasticity than the other two, we witnessed a negligible difference in deformation between the clay types. Also, the surface finish varied depending on the type, with terracotta yielding the cleanest finish (Fig. 9). Terracotta stains the concrete, exposing a trace of its fabrication and creating a connection between the geometry and material articulation of the formwork. Thus, we ultimately picked terracotta clay as the formwork material for the rest of the experiments.

Keeping the diameter as 100 mm, an increased print height of 450 mm in the preliminary studies necessitated introducing an incremental casting process to reduce the formwork deformation; we will

Fig. 8. From left to right: prints with 3 mm, 1 mm, and 2 mm bead heights.

Fig. 9. From left to right: RO-95 Cone 6 Porcelain, RO-01 You Betcha Mix High Fire White Clay, and RO-82M Terracotta with Fine Grog [49].

discuss this in the next section, where we perform a rigorous testing process to tune various factors for controlling clay deformation.

2.3.2. Deformation control

We used an incremental casting process inspired by SDC [32] by pouring concrete in several steps, which allowed the earlier casts to begin curing as we poured the following sections. The last two pours bond without affecting the earlier sections. Fig. 10 shows a schematic of four pours; after the first print of clay, we cast concrete, then print the second section of the clay and cast concrete (with about a 20 m interval from the first cast). The first two casts bond as the concrete has only partially cured. A similar process occurs with the third and second layers while not affecting the first, helping control the lateral hydrostatic pressure from the wet concrete, thus limiting deformations. We controlled the curing process by adding and adjusting the accelerator magnitude in the GFRC mixture. In this study phase, we explored a balance of factors such as the accelerator amount, pour height, cylinder diameter, and timing between the casting sections.

The control of hydrostatic pressure from the wet concrete on the formwork wall during the casting is the primary driver for this set of experiments to create taller samples. The higher casting height inserts more lateral pressure on the wet clay wall, causing more deformation. The incremental formwork printing and concrete casting with limited pour heights help control this pressure. Larger print cross sections can also produce more deformations as increasing the diameter of the cylinders causes additional circumferential hoop stress [59], therefore, more lateral displacements in the formwork. Fig. 11 shows samples of the testing procedure for casting cylinders of various heights and

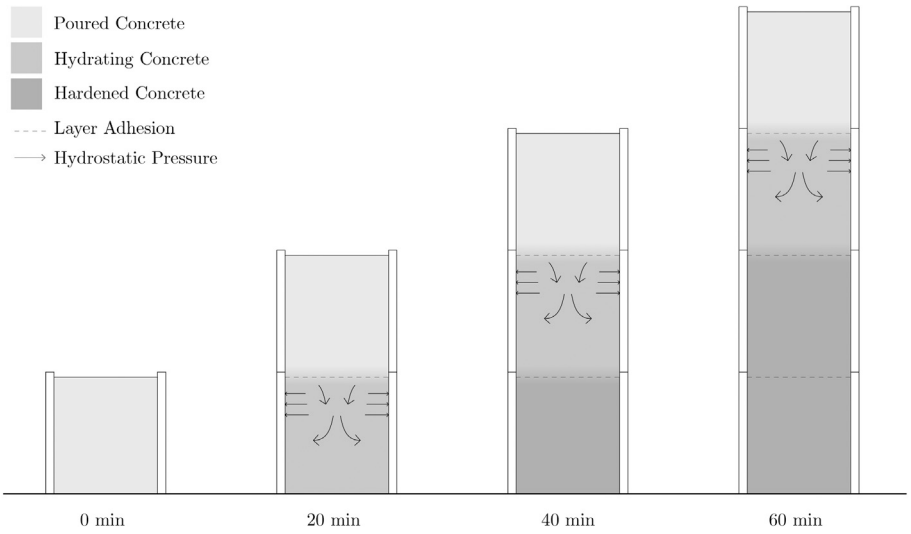

Fig. 10. Schematic of the casting sequence and underlying actions.

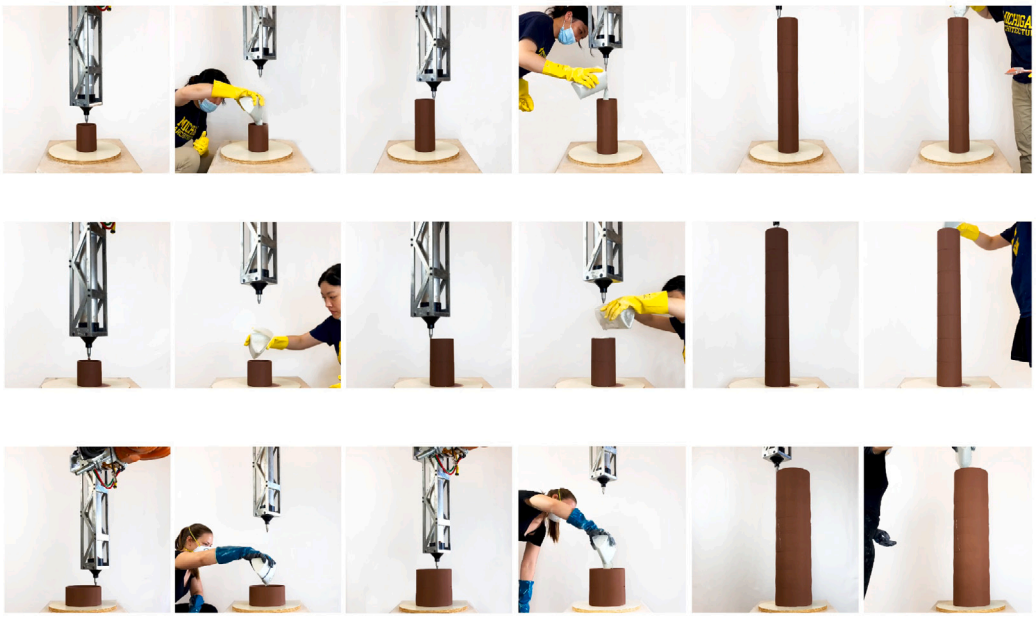

Fig. 11. Samples of the testing procedure to investigate print/cast height, accelerator, timing, and cylinder diameter (from top to bottom row): six casts of 135 mm with 100 mm diameter, eight casts of 100 mm with 100 mm diameter, and eight casts of 100 mm with 200 mm diameter.

diameters, showing the first two casts and the last cast for each testing scenario.

Since the investigation of the hoop stress's effect on deformations during the casting process is out of the scope of this paper, we continued the experiments with prints of 100 mm diameter. We tested 100 mm and 135 mm pour heights and used the GFRC mixture (Section 2.1.2) in combination with 0, 20, and 30 grams of accelerator (Table 1) for deformation comparisons. The accelerator amount is selected to consider tube changing, printing time, and casting intervals. So, the fabrication setup and the concrete curing speed are essential for timing between the casts. As the clay tube capacity is limited to the maximum continuous print of 250 m, we required at least 15 min between the casts to disassemble the extruder and replace it with a full tube. The total height of the cylindrical columns was 800 mm for 100 mm and 810 mm for 135 mm section heights. The experimentation of this phase helped find a proper balance between the timing, mixture, and section heights.

3. Results and discussion

3.1. Experimental findings

Fig. 12 shows the selected resulting specimens and their deformation map from the deformation control tests with 100 mm and 135 mm print and casting heights; we evidenced no formwork failure with six pours of 135 mm and eight pours of 100 mm with both 20 and 30 grams of the accelerator. Increasing the accelerator from 20 to 30 grams with 135 pour heights reduced the deformations significantly, although it produced less layer adhesion. Lowering the pour heights to 100 mm with 20 grams of accelerator helped reduce the deformations

Table 1
Concrete mix formulations (grams per liter of mixture).

Cement	Silica fume	Ground silica	Water	Accelerator	Polymer	Super plasticizer	Fine sand	Glass fiber
1125	150	300	390	0	75	15	1125	45
1125	150	300	390	20	75	15	1125	45
1125	150	300	390	30	75	15	1125	45
1125	150	300	350	20	75	15	1125	45

Fig. 12. Deformation control test results (left figure) and the circumferential change (right figure): (from left to right cylinder) 100 mm pour height, 20 g acc; 100 mm pour height, 20 g acc; 100 mm pour height, 30 g acc; 135 mm pour height, 30 g acc; and 135 mm pour height, 20 g acc.

by maintaining the layer adhesion. We repeated the experiment with 100 mm pour heights and 20 grams of accelerator three times to confirm the consistency of deformations in the resulting specimens and the replicability of the process. The deformations are measured by the change in circumference of the concrete using a soft tape measure after demolding the specimens (Fig. 12).

The results of this experimentation set up a framework for applying this process to different geometries; we will present a case study in the next section, where we test and adjust the process to create a complex form.

3.2. The Cocoon

The final phase of the study considered factors such as ease of fabrication, scalability, and customization of the process to prove the technique's viability. The Cocoon (Fig. 1), resulting from this final investigation, showcases the potential of the intricate detail, undercuts, and openings, accommodating nonlinear surfaces.

The Scherk surface (named after Heinrich Scherk) is an example of a minimal surface showing the smallest possible area for spanning its boundary [60]. Scherk described two completely embedded minimal surfaces in 1834; a doubly and a singly periodic surface. The surfaces can have many iterations according to the number of saddle branches and holes, turns around the axis, and bends towards the axis. The geometrical revolving between branches and voids and the variety of designs could provide an appropriate baseline to test our proof of concept for complex shapes. The topology of this case study is a Scherk-Collins surface generated by Carlo H. Séquin for Sculpture Generator 1 at UC Berkeley [61].

We generated a continuous Helix toolpath (Fig. 13) for each section of the Scherk surface using Grasshopper, a visual algorithmic editor integrated into Rhinoceros's 3D modeling framework [56]. Integrating the toolpath into the SMT allows the clay extruder to follow the designed toolpath while continuing to extrude clay through the nozzle.

To prevent clay's deformation during concrete casting caused by hydrostatic pressure, we considered a few supporting scenarios (Fig. 14); (1) Void Filled: is where the toolpath lines are parallel to each other in the void area of the structure. It forms a dense double-layered clay wall during clay printing to prevent concrete from leaking on both sides of the branches. It also creates a continuous clay extrusion path while switching between the branches. (2) Void Support: is the extra rib added to the void area during printing. It works with the Void Filled to reinforce the print center. (3) Rib Support: is the rib added to the end of each branch to improve the formwork's overhang functionality and prevent concrete leaking and clay deformation. The Rib Support conserves the clay and reduces the printing time by providing the necessary reinforcement instead of printing two layers around the circumference.

The pour heights were adjusted from 100 mm to 50 mm between the casts to reduce the deformations (Fig. 15). The case study's incremental clay printing and concrete casting consisted of 13 prints with 26 consecutive concrete pours resulting in a 1.3 m height element. This process took about 9 h to complete the print and cast the Cocoon element with the dimensions 1300 mm × 267 mm × 267 mm and a wall thickness of 33 mm. The developed supporting systems created no break or overlap on the printing path, avoiding seam creation and a system vulnerable to failure. The successful fabrication of this case study demonstrated a viable process and potential for further application and adjustment of this method to create large-scale complex geometries.

3.3. Discussion

The cylindrical tests informed the initial phases of the physical prototyping to investigate the clay types, bead heights, and the effect of concrete hydrostatic pressure on the incremental formwork printing and concrete casting process. The results of the cylindrical tests can be summarized as follows; (1) there was no significant difference in the formwork deformation between the three clay types, (2) the 1 mm bead

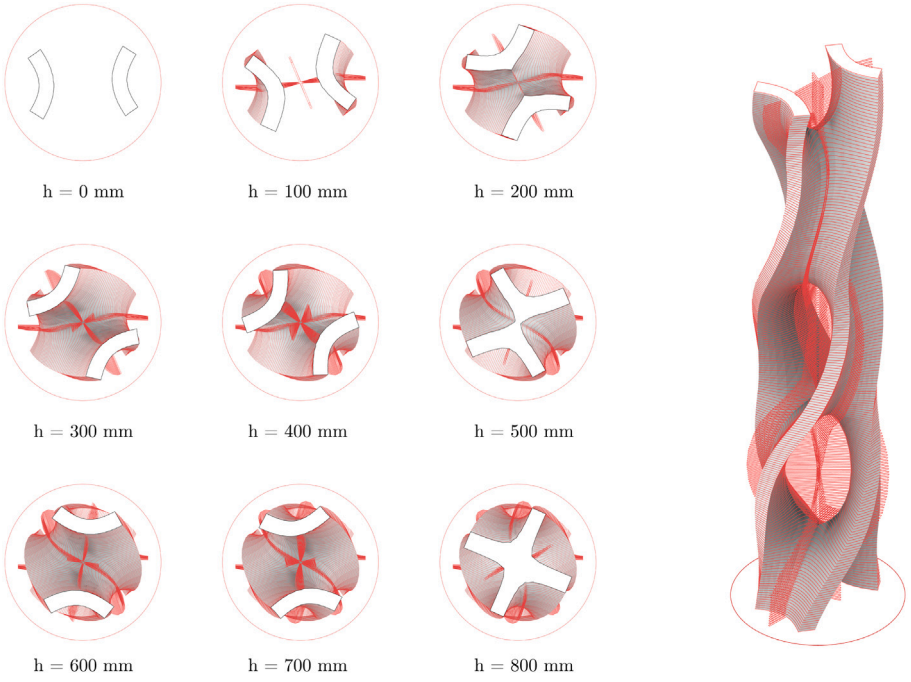

Fig. 13. Plan of toolpath generation displaying the support structure based on geometry.

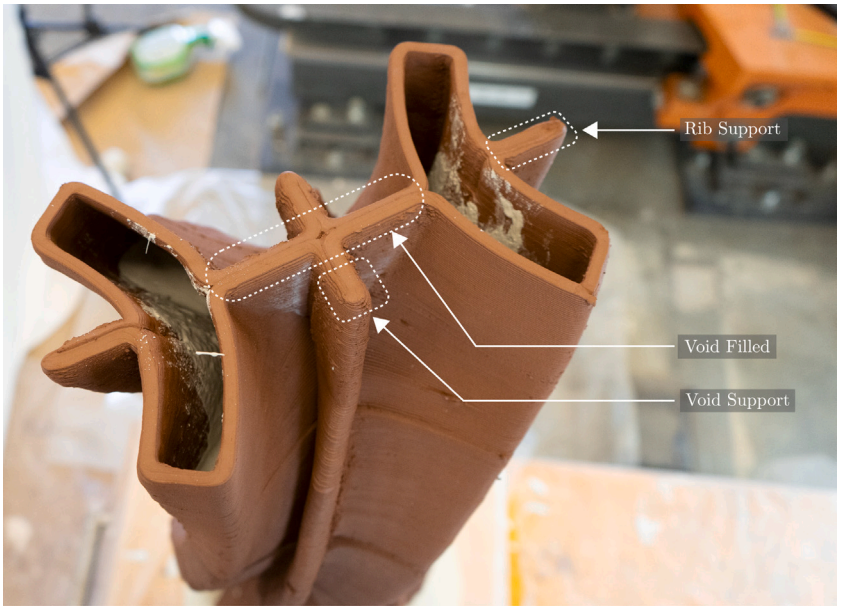

Fig. 14. Added supports facilitating the clay printing and concrete casting of the complex Cocoon element.

height produced the smallest deformations and the lowest concrete surface porosity, (3) the increase in the print height or section diameter caused larger deformations, and (4) accelerator amounts of greater than 20 g resulted in poor layer adhesion between the concrete casts.

As a result of the preliminary explorations, we achieved minimal deformations by limiting the section heights to 100 mm, the accelerator to 20 g, and the casting intervals to 20 min while maintaining layer adhesion between each cast. However, these preliminary tests did not validate the technique's viability for achieving larger scales with customized and complex forms. Therefore, the final experiments investigated improvements such as creating a minimal surface with openings and various formwork supports.

The minimal surface formwork in the initial prototypes failed due to relatively large deformations during concrete casting, making tall overhangs and pour heights unachievable. The hydrostatic pressure of concrete created a sunken vessel on the formwork exterior and pushed the clay to failure. Therefore, the continuation of the tests necessitated the addition of ribbed supports to the extruded clay to avoid excessive deformations. The ribs helped maintain the curved form's consistency and rigidity and allowed opening integration. Moreover, instead of 100 mm increments for concrete casting, we reduced pour heights to 50 mm (Fig. 15). Still, we kept the clay extrusion to 100 mm segments with casting intervals at about 20 min, and maintained the accelerator amount at 20 g.

With the Cocoon case study, we could achieve a total height of 1.3 m in about 9 h without any failure, although we did not explore the maximum reachable height. However, based on the empirical results,

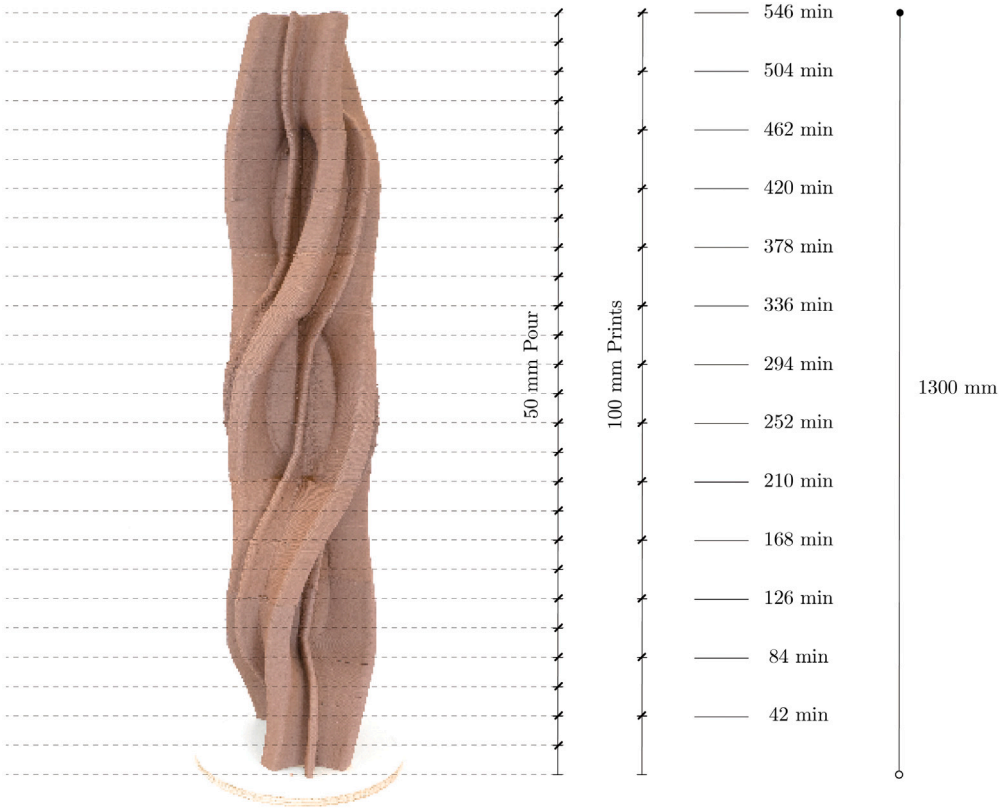

Fig. 15. Print and pour heights for printing the 1.3 m structure in 9 h and 6 min.

we could potentially cast taller columns as long as (1) fabrication constraints such as tool orientation and position in the working envelope allow, (2) a proper casting and printing sequence is followed, (3) the accelerator is tuned if required, and (4) the deformation failure of the wet clay or curing concrete does not occur due to the increasing pressure and weight. A more in-depth investigation of the material properties of the fresh clay and curing concrete and the study of their interaction is required to quantify this possibility.

4. Conclusions

The presented technique enabled using a low-cost material with low environmental impact as formwork for creating concrete elements of bespoke shapes. Using clay reduces the carbon footprint of creating complex forms by minimizing material waste and providing recycling opportunities. The developed incremental printing and casting process allowed previously unachievable scales by having the clay and concrete work together. The technique also enabled the integration of openings and overhangs, which was made easier through the effortless demolding process avoiding the constraints of concrete and polymer formwork extrusion. Overall, the technique sought to challenge conventional methods and materials for 3D-printed formworks, demonstrating the ability to reduce the environmental impacts of concrete construction without compromising the complexity and time efficiency of bespoke elements. The following section will present the limitations and suggest potential areas for further investigation.

4.1. Limitations and future research

The current fabrication setup provided the opportunity to achieve the initial goals of the research; however, it needs to be improved in scale. The clay tube capacity was limited, requiring frequent tube changes, which slowed down the large-scale production process. The recently developed technologies for large-scale earth-printing using a continuous pumping system [62,63] provide an easier way to produce building-scale elements. The fabrication setup can then be extended to a multi-robotic cooperative workcell by situating the print bed between two industrial robotic arms (Fig. 16). The robots will be equipped with two pumping systems feeding the extruder for clay printing and pumping concrete into the formwork using a tool that can mix accelerator into the concrete at the nozzle providing a more continuous process.

The existing computational design framework did not include structural analysis. Accordingly, the digital fabrication process did not consider the integration of reinforcing bars to improve the structural performance of the elements. To move the research towards feasible production of reinforced concrete building components for real-world projects, the process requires considering structural performance and integrating reinforcing strategies (such as conventional bars [13] or a rod bending technique [47]) into the fabrication process. Combined with experimental load tests, these results will be compared to traditional concrete casting methods and help develop mechanical models for more precise structural performance predictions.

More advanced research is required to investigate wet clay's underlying physics and behavior under lateral stress from fresh concrete [64,65], as well as the interactions between the two materials. This necessitates precise measurements of clay plasticity, density, shrinkage, absorption, water content, and rheological properties. Also, the effect of print pressure, speed, nozzle size, and pumping on the rheological characteristics of the clay should be studied. Furthermore, the effect of using accelerator admixtures on layer adhesion, porosity, material properties, and structural performance of concrete should be carefully examined.

Other potential improvements include in-depth research on the concrete mixture (e.g. using a less carbon-intensive mix with larger or recycled aggregates [45,66]), as well as the integration of optimization scenarios into the computational design framework, such as material minimization algorithms and optimal shape design for the rib and void supporting systems.

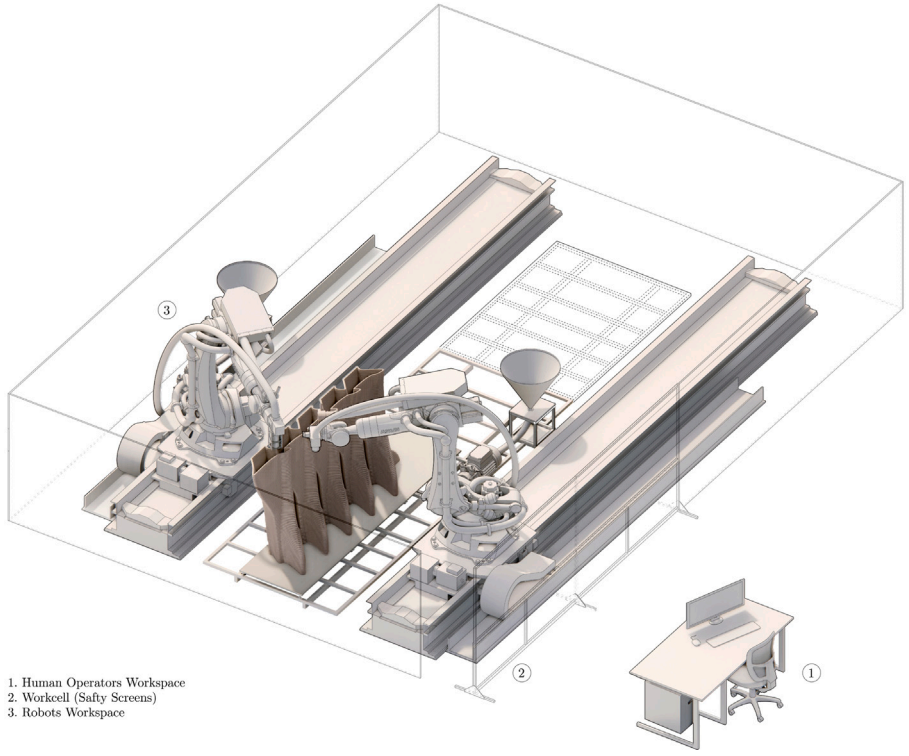

Fig. 16. Schematic of the digital fabrication setup; one robot prints the clay, and the other pumps the concrete mix.

Declaration of competing interest

The authors declare that they have no known competing financial interests or personal relationships that could have appeared to influence the work reported in this paper.

Data availability

No data was used for the research described in the article.

Acknowledgments

The presented study was conducted as a Capstone project of the Master of Science Digital and Material Technologies at Taubman College. We want to thank Prof. Tsz Yan Ng for providing the formulation for the base concrete mixture and her guidance in tuning the accelerator admixture. We also thank many others who were, directly and indirectly involved in the project, particularly Asa Peller, Mark Meier, Austin Wiskur, and Alyssa Fellabaum.

Funding

The research was supported by the A. Alfred Taubman College of Architecture and Urban Planning and the Rackham Graduate School at the University of Michigan.

References

[1] T. Abergel, J. Dulac, I. Hamilton, M. Jordan, A. Pradeep, Global status report for buildings and construction—towards a zero-emissions, efficient and resilient buildings and construction sector, in: Environment Programme, United Nations Environment Programme, 2019, https://www.unep.org/resources/publication/2019-global-status-report-buildings-and-construction-sector. (Accessed 14 April 2023).

[2] P.J. Monteiro, S.A. Miller, A. Horvath, Towards sustainable concrete, Nature Mater. 16 (7) (2017) 698–699, http://dx.doi.org/10.1038/nmat4930.

[3] H. Schipper, S. Grünewald, Efficient material use through smart flexible formwork method, in: International Symposium on Environmentally Friendly Concrete, ECO-Crete, 2014, http://resolver.tudelft.nl/uuid:5f767d7f-6ad1-4e37-9efc-1817e9561274.

[4] F. Antony, R. Grießhammer, T. Speck, O. Speck, Sustainability assessment of a lightweight biomimetic ceiling structure, Bioinspiration Biomim. 9 (1) (2014) 016013, http://dx.doi.org/10.1088/1748-3182/9/1/016013.

[5] J. Burger, E. Lloret-Fritschi, F. Scotto, T. Demoulin, L. Gebhard, J. Mata-Falcón, F. Gramazio, M. Kohler, R.J. Flatt, Eggshell: ultra-thin three-dimensional printed formwork for concrete structures, 3D Print. Addit. Manuf. 7 (2) (2020) 48–59, http://dx.doi.org/10.1089/3dp.2019.0197.

[6] T. Wangler, N. Roussel, F.P. Bos, T.A. Salet, R.J. Flatt, Digital concrete: a review, Cem. Concr. Res. 123 (2019) 105780, http://dx.doi.org/10.1016/j.cemconres.2019.105780.

[7] A. Kudless, J. Zabel, C. Naeve, T. Florian, The design and fabrication of confluence park, in: Fabricate 2020: Making Resilient Architecture, JSTOR, 2020, http://dx.doi.org/10.2307/j.ctv13xpsvw.8.

[8] N. Hack, W.V. Lauer, Mesh-mould: robotically fabricated spatial meshes as reinforced concrete formwork, Archit. Des. 84 (3) (2014) 44–53, http://dx.doi.org/10.1002/ad.1753.

[9] E. Lloret, A.R. Shahab, M. Linus, R.J. Flatt, F. Gramazio, M. Kohler, S. Langenberg, Complex concrete structures: Merging existing casting techniques with digital fabrication, Comput. Aided Des. 60 (2015) 40–49, http://dx.doi.org/10.1016/j.cad.2014.02.011.

[10] A. Søndergaard, J. Feringa, T. Nørbjerg, K. Steenstrup, D. Brander, J. Graversen, S. Markvorsen, A. Bærentzen, K. Petkov, J. Hattel, et al., Robotic hot-blade cutting: An industrial approach to cost-effective production of double curved concrete structures, in: Robotic Fabrication in Architecture, Art and Design 2016, Springer, 2016, pp. 150–164, http://dx.doi.org/10.1007/978-3-319-26378-6_11.

[11] T.A. Salet, Z.Y. Ahmed, F.P. Bos, H.L. Laagland, Design of a 3D printed concrete bridge by testing, Virtual Phys. Prototyp. 13 (3) (2018) 222–236, http://dx.doi.org/10.1080/17452759.2018.1476064.

[12] P.F. Martins, P.F. de Campos, S. Nunes, J.P. Sousa, The tectonics of digitally fabricated concrete. A case for robotic hot wire cutting, in: RILEM International Conference on Concrete and Digital Fabrication, Springer, 2018, pp. 311–322, http://dx.doi.org/10.1007/978-3-319-99519-9_29.

[13] L. Gebhard, J. Burger, J. Mata-Falcón, E. Lloret Fritschi, F. Gramazio, M. Kohler, W. Kaufmann, Towards efficient concrete structures with ultra-thin 3D printed formwork: exploring reinforcement strategies and optimisation, Virtual Phys. Prototyp. 17 (3) (2022) 599–616, http://dx.doi.org/10.1080/17452759.2022.2041873.

[14] XtreeE, 2023, https://xtreee.com. (Accessed 14 April 2023).

[15] Branch Technology, 2023, https://branchtechnology.com. (Accessed 14 April 2023).

[16] Ai Build, 2023, https://ai-build.com. (Accessed 14 April 2023).

[17] Apis Cor, 2023, https://www.apis-cor.com. (Accessed 14 April 2023).

[18] B. Khoshnevis, D. Hwang, K.T. Yao, Z. Yeh, Mega-scale fabrication by contour crafting, Int. J. Ind. Syst. Eng. 1 (3) (2006) 301–320, http://dx.doi.org/10.1504/IJISE.2006.009791.

[19] M.S. Khan, F. Sanchez, H. Zhou, 3-D printing of concrete: beyond horizons, Cem. Concr. Res. 133 (2020) 106070, http://dx.doi.org/10.1016/j.cemconres.2020.106070.

[20] F. Bos, R. Wolfs, Z. Ahmed, T. Salet, Large scale testing of digitally fabricated concrete (DFC) elements, in: RILEM International Conference on Concrete and Digital Fabrication, Springer, 2018, pp. 129–147, http://dx.doi.org/10.1007/978-3-319-99519-9_12.

[21] A. Anton, P. Bedarf, A. Yoo, B. Dillenburger, L. Reiter, T. Wangler, R.J. Flatt, Concrete choreography: Prefabrication of 3D-printed columns, Fabricate 2020: Making Resilient Architecture (2020) 286–293, http://dx.doi.org/10.2307/j.ctv13xpsvw.41.

[22] B. Zareiyan, B. Khoshnevis, Effects of interlocking on interlayer adhesion and strength of structures in 3D printing of concrete, Autom. Constr. 83 (2017) 212–221, http://dx.doi.org/10.1016/j.autcon.2017.08.019.

[23] A. Siddika, M.A.A. Mamun, W. Ferdous, A.K. Saha, R. Alyousef, 3D-printed concrete: Applications, performance, and challenges, J. Sustain. Cem.-Based Mater. 9 (3) (2020) 127–164, http://dx.doi.org/10.1080/21650373.2019.1705199.

[24] V. Vaitkevičius, E. Šerelis, V. Kerševičius, Effect of ultra-sonic activation on early hydration process in 3D concrete printing technology, Constr. Build. Mater. 169 (2018) 354–363, http://dx.doi.org/10.1016/j.conbuildmat.2018.03.007.

[25] J. Xiao, C. Wang, T. Ding, A. Akbarnezhad, A recycled aggregate concrete high-rise building: Structural performance and embodied carbon footprint, J. Clean. Prod. 199 (2018) 868–881, http://dx.doi.org/10.1016/j.jclepro.2018.07.210.

[26] M.K. Mohan, A. Rahul, G. De Schutter, K. Van Tittelboom, Extrusion-based concrete 3D printing from a material perspective: A state-of-the-art review, Cem. Concr. Compos. 115 (2021) 103855, http://dx.doi.org/10.1016/j.cemconcomp.2020.103855.

[27] W. McGee, J. Feringa, A. Søndergaard, Processes for an architecture of volume: robotic wire cutting, in: Robotic Fabrication in Architecture, Art, and Design (ROB|ARCH), Springer, 2013, pp. 62–71, http://dx.doi.org/10.1007/978-3-7091-1465-0_5.

[28] A. Jipa, B. Dillenburger, 3D printed formwork for concrete: state-of-the-art, opportunities, challenges, and applications, 3D Printing and Additive Manufacturing (2021) http://dx.doi.org/10.1089/3dp.2021.0024.

[29] N. Hack, K. Dörfler, A.N. Walzer, T. Wangler, J. Mata-Falcón, N. Kumar, J. Buchli, W. Kaufmann, R.J. Flatt, F. Gramazio, et al., Structural stay-in-place formwork for robotic in situ fabrication of non-standard concrete structures: A real scale architectural demonstrator, Autom. Constr. 115 (2020) 103197, http://dx.doi.org/10.1016/j.autcon.2020.103197.

[30] G. Gardiner, SFMOMA Façade: Advancing the Art of High-Rise FRP, CompositesWorld, 2015, https://www.compositesworld.com/articles/sfmoma-faade-advancing-the-art-of-high-rise-frp. (Accessed 14 April 2023).

[31] T. Maharana, Y. Negi, B. Mohanty, Review article: Recycling of polystyrene, Polym.-Plast. Technol. Eng. 46 (7) (2007) 729–736, http://dx.doi.org/10.1080/03602550701273963.

[32] E. Lloret-Fritschi, F. Scotto, F. Gramazio, M. Kohler, K. Graser, T. Wangler, L. Reiter, R.J. Flatt, J. Mata-Falcón, Challenges of real-scale production with smart dynamic casting, in: RILEM International Conference on Concrete and Digital Fabrication, Springer, 2018, pp. 299–310, http://dx.doi.org/10.1007/978-3-319-99519-9_28.

[33] B. Peters, Additive formwork: 3D printed flexible formwork, in: Annual Conference of the Association of Computer Aided Design in Architecture, CUMINCAD, 2014, http://dx.doi.org/10.52842/conf.acadia.2014.517.

[34] M. Leschok, B. Dillenburger, Dissolvable 3DP formwork: Water-dissolvable 3D printed thin-shell formwork for complex concrete components, in: Annual Conference of the Association of Computer Aided Design in Architecture, CUMINCAD, 2019, http://dx.doi.org/10.52842/conf.acadia.2019.188.

[35] A. Jipa, M. Bernhard, B. Dillenburger, Submillimeter formwork: 3D-printed plastic formwork for concrete elements, in: TxA 78th Annual Conference and Design Expo, 2017, http://dx.doi.org/10.3929/ethz-b-000237359.

[36] R. Naboni, L. Breseghello, Fused deposition modelling formworks for complex concrete constructions, in: Conference of the Iberoamerican Society of Digital Graphics, SIGraDi, CUMINCAD, 2018, http://dx.doi.org/10.5151/sigradi2018-1648.

[37] T. Huber, J. Burger, J. Mata-Falcón, W. Kaufmann, Structural design and testing of material optimized ribbed rc slabs with 3D printed formwork, Structural Concrete 24 (2) (2023) 1932–1955, http://dx.doi.org/10.1002/suco.202200633.

[38] J. Burger, T. Wangler, Y.-H. Chiu, C. Techathuvanun, F. Gramazio, M. Kohler, E. Lloret-Fritschi, Material-informed formwork geometry-the effects of cross-sectional variation and patterns on the strength of 3D printed eggshell formworks, in: Education and Research in Computer Aided Architectural Design in Europe, eCAADe, CUMINCAD, 2021, http://dx.doi.org/10.52842/conf.ecaade.2021.2.199.

[39] J. Pakkanen, D. Manfredi, P. Minetola, L. Iuliano, About the use of recycled or biodegradable filaments for sustainability of 3D printing, in: International Conference on Sustainable Design and Manufacturing, Springer, 2017, pp. 776–785, http://dx.doi.org/10.1007/978-3-319-57078-5_73.

[40] B. Khoshnevis, S. Bukkapatnam, H. Kwon, J. Saito, Experimental investigation of contour crafting using ceramics materials, Rapid Prototyp. J. (2001) http://dx.doi.org/10.1108/13552540110365144.

[41] B. Gürsoy, From control to uncertainty in 3D printing with clay, in: Education and Research in Computer Aided Architectural Design in Europe, CUMINCAD, 2018, http://dx.doi.org/10.52842/conf.ecaade.2018.2.021.

[42] S. Wang, Z. Xuereb Conti, F. Raspall, Optimization of clay mould for concrete casting using design of experiments, in: Association for Computer-Aided Architectural Design Research in Asia (CAADRIA) Conference, CUMINCAD, 2019, http://dx.doi.org/10.52842/conf.caadria.2019.2.283.

[43] S. Wang, S. Dritsas, P. Morel, K. Ho, Clay robotics: A hybrid 3D printing casting process, in: Challenges for Technology Innovation: An Agenda for the Future, CRC Press, 2017, pp. 83–88, http://dx.doi.org/10.1201/9781315198101.

[44] M. Bruce, G. Clune, R. Xie, S. Mozaffari, A. Adel, Cocoon: 3D printed clay formwork for concrete casting, in: Annual Conference of the Association of Computer Aided Design in Architecture, CUMINCAD, 2021, pp. 400–409, http://dx.doi.org/10.7302/7046.

[45] S. Zou, J. Xiao, T. Ding, Z. Duan, Q. Zhang, Printability and advantages of 3D printing mortar with 100% recycled sand, Constr. Build. Mater. 273 (2021) 121699, http://dx.doi.org/10.1016/j.conbuildmat.2020.121699.

[46] G. Vantyghem, W. De Corte, E. Shakour, O. Amir, 3D printing of a post-tensioned concrete girder designed by topology optimization, Autom. Constr. 112 (2020) 103084, http://dx.doi.org/10.1016/j.autcon.2020.103084.

[47] A. Mirjan, J. Mata-Falcón, C. Rieger, J. Herkrath, W. Kaufmann, F. Gramazio, M. Kohler, Mesh mould prefabrication, in: RILEM International Conference on Concrete and Digital Fabrication, Springer, 2022, pp. 31–36, http://dx.doi.org/10.1007/978-3-031-06116-5_5.

[48] E. Lloret-Fritschi, E. Quadranti, F. Scotto, L. Fuhrimann, T. Demoulin, S. Mantellato, L. Unteregger, J. Burger, R.G. Pileggi, F. Gramazio, et al., Additive digital casting: From lab to industry, Materials 15 (10) (2022) 3468, http://dx.doi.org/10.3390/ma15103468.

[49] Rovin ceramics, 2023, https://rovinceramics.com/. (Accessed 14 April 2023).

[50] H.B. Seed, R.J. Woodward Jr, R. Lundgren, Clay mineralogical aspects of the atterberg limits, J. Soil Mech. Found. Div. 90 (4) (1964) 107–131, http://dx.doi.org/10.1061/JSFEAQ.0000628.

[51] J. Bilotti, B. Norman, D. Rosenwasser, J. Leo Liu, J.E. Sabin, Robosense 2.0. Robotic sensing and architectural ceramic fabrication, in: Conference of the Association for Computer Aided Design in Architecture, CUMINCAD, 2018, pp. 18–20, http://dx.doi.org/10.52842/conf.acadia.2018.276.

[52] A. Ruscitti, C. Tapia, N. Rendtorff, A review on additive manufacturing of ceramic materials based on extrusion processes of clay pastes, Cerâmica 66 (2020) 354–366, http://dx.doi.org/10.1590/0366-69132020663802918.

[53] S. Hotoon, Progressing cavity pump guide and design, 2023, https://www.northridgepumps.com/article-220_progressing-cavity-pump-guide-and-design. (Accessed 14 April 2023).

[54] D. Pigram, W. McGee, Formation embedded design, in: Conference of the Association for Computer Aided Design in Architecture, 2011, pp. 122–131, http://dx.doi.org/10.52842/conf.acadia.2011.122.

[55] Microsoft, A tour of the C# language, 2023, https://learn.microsoft.com/en-us/dotnet/csharp/tour-of-csharp/. (Accessed 14 April 2023).

[56] R. McNeel, et al., Rhinoceros: NURBS modleing for windows, 2020, https://www.rhino3d.com/. (Accessed 14 April 2023).

[57] KUKA robot language, 2023, https://www.kuka.com/en-de/services/engineering/application-and-robot-programming. (Accessed 14 April 2023).

[58] EtherCAT technology group, 2023, https://www.ethercat.org. (Accessed 14 April 2023).

[59] D. Roylance, Pressure vessels, mechanics of materials (lecture notes), 2001, https://web.mit.edu/course/3/3.11/www/modules/pv.pdf. (Accessed 14 April 2023).

[60] Scherk's minimal surface, 2015, https://wewanttolearn.wordpress.com/2015/11/11/scherks-minimal-surface/. (Accessed 14 April 2023).

[61] Scherk-collins sculpture generator, 2023, https://people.eecs.berkeley.edu/~sequin/SCULPTS/scherk.html. (Accessed 14 April 2023).

[62] M. Gomaa, W. Jabi, A.V. Reyes, V. Soebarto, 3D printing system for earth-based construction: Case study of cob, Autom. Constr. 124 (2021) 103577, http://dx.doi.org/10.1016/j.autcon.2021.103577.

[63] O. Kontovourkis, G. Tryfonos, Robotic 3D clay printing of prefabricated non-conventional wall components based on a parametric-integrated design, Autom. Constr. 110 (2020) 103005, http://dx.doi.org/10.1016/j.autcon.2019.103005.

[64] G. Ovarlez, N. Roussel, A physical model for the prediction of lateral stress exerted by self-compacting concrete on formwork, Mater. Struct. 39 (2006) 269–279, http://dx.doi.org/10.1617/s11527-005-9052-1.

[65] A. Perrot, A. Pierre, S. Vitaloni, V. Picandet, Prediction of lateral form pressure exerted by concrete at low casting rates, Mater. Struct. 48 (7) (2015) 2315–2322, http://dx.doi.org/10.1617/s11527-014-0313-8.

[66] R.J. Flatt, T. Wangler, On sustainability and digital fabrication with concrete, Cem. Concr. Res. 158 (2022) 106837, http://dx.doi.org/10.1016/j.cemconres.2022.106837.